PROCEEDINGS OF SCIENCE

Systematic uncertainty in the analysis of the TA fluorescence detector from fluorescence yield models

Kohei Komori,[a,*] **Yuichiro Tameda,**[a] **Shoma Sato,**[a] **Yutaro Takagi,**[a] **Yuki Kusumori,**[a] **Hirai Iwagami,**[a] **Shoichi Ogio,**[b] **Keitaro Fujita,**[b] **Takayuki Tomida**[c] **and for the Telescope Array Collaboration**

[a] *Graduate School of Engineering , Osaka Electro-Communication University, 18-8, Hastutyo, Neyagawa-shi, Osaka, 572-0833, Japan*

[b] *Institute for Cosmic Ray Research, the University of Tokyo, 5 chome 1-5, kashiwanoha, Kashiwa-shi, Chiba, 277-0882, Japan*

[c] *Academic Assembly School of Science and Technology Institute of Engineering, Shinshu University, 3 chome 1-1, asahi, Matsumoto-shi, Nagano, 390-8621, Japan*

E-mail: me23a007@oecu.jp, tameda@osakac.ac.jp

Currently, ultra-high energy cosmic rays (UHECRs) are being measured by the Telescope Array (TA) and Pierre Auger (Auger) experiments. There are differences in the energy spectra measured by TA and Auger. One reason for this difference is systematic uncertainty in the energy determination. The fluorescence yield model, which consists of fluorescence emission efficiencies and spectra, is one of the most significant components of this systematic uncertainty. Fluorescence emission efficiencies and spectra have been measured by various experiments, and different measurements are currently used to determine the energy of the TA and Auger experiments. In this study, we estimate the influence of the fluorescence yield model on the systematic uncertainty in the energy determination of the TA fluorescence detector.

38th International Cosmic Ray Conference (ICRC2023)
26 July - 3 August, 2023
Nagoya, Japan

ICRC2023
38th International Cosmic Ray Conference
The Astroparticle Physics Conference

*Speaker

PoS(ICRC2023)330

1. Introduction

In this study, we estimate the influence of the fluorescence yield model on the systematic uncertainty in the energy determination of the Telescope Array (TA) fluorescence detector. TA and Pierre Auger are the largest cosmic ray experiments in the northern and southern hemispheres, respectively. The TA experiment is being conducted in the desert area of Millard County, Utah, USA. This experiment consists of 507 surface particle detectors arranged in a grid with 1.2 km intervals, surrounded by three stations with FD 20 – 30 km apart. The Auger experiment is being conducted near the town of Marargue, Mendoza Province, Argentina. This experiment consists of 1,660 water Cherenkov detectors arranged in a triangular grid with a spacing of 1.5 km, surrounded by four stations with FDs.

One of the results obtained from the UHECRs measured by the above two experiments is the energy spectrum, and a difference is observed. The energy spectra of the TA and Auger experiments are shown in Figure 1 (a). The flux measured by the Auger experiment is lower than that measured by TA. One reason for this difference between two spectra is systematic uncertainty in the energy determination. The fluorescence yield model, which consists of fluorescence emission efficiencies and spectra, is one of the most significant components of this systematic uncertainty.

The fluorescence model is used to estimate the amount of fluorescence yield from particles produced by the air shower phenomenon. Fluorescence yield, one of the components of the fluorescence model, is the amount of light emitted per MeV of energy loss. The fluorescence yields measured in each experiment is shown below (Figure 1 (b)). Fluorescence yield varies from experiment to experiment. The other component, the fluorescence spectrum, is the intensity distribution of fluorescence generated in each wavelength band. Fluorescence spectra of FLASH used by TA and Airfly used by Auger are shown in Figure 1 (c) and (d), respectively. Thus, fluorescence emission efficiencies and spectra have been measured by various experiments, and different measurements are currently used to determine the energy of the TA and Auger experiments. In this study, we estimate the influence of the fluorescence yield model on the systematic uncertainty in the energy determination of the TA fluorescence detector.

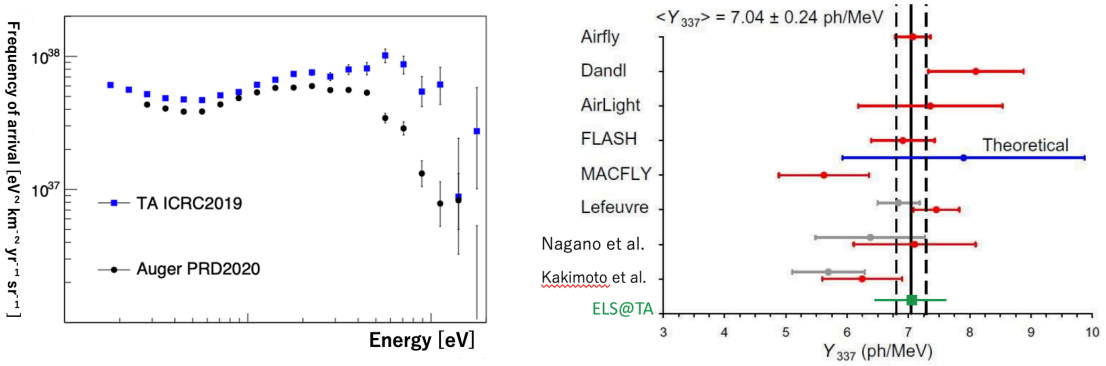

Figure 1: Left: The flux as a function of energy as measured by TA and Auger. Right: Various measurements and calculations of the fluorescence yield. [1]

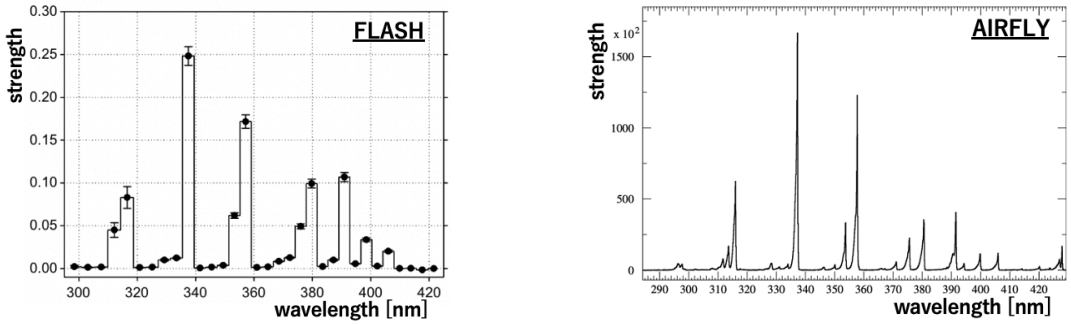

Figure 2: Left: The fluorescence spectrum as measured by FLASH. Right: The fluorescence spectrum as measured by AIRFLY. The vertical axis is standardized and the horizontal axis is wavelength

2. Energy determination for each fluorescence model

In order to estimate the systematic uncertainty in the energy determination due to each fluorescence model, we first run simulations at 10^{18} eV, 10^{19} eV, and 10^{20} eV using the standard fluorescence model. Next, monocular reconstruction is performed for each fluorescence model. Next, event selection is applied to the result of monocular reconstruction. The shower profile is reconstructed with the geometry given by the simulation to remove the influence of the geometry reconstruction on the remaining events in the event selection. The above procedure is performed for each fluorescence model to estimate the energy determination. The details are described below.

In the simulation, after the primary cosmic rays enter the atmosphere, a large number of secondary particles are produced by the air shower phenomenon, and the fluorescence emitted from the secondary particles is measured by FD in the TA experiment. The atmospheric conditions used in the simulations are the US standard atmosphere [10]. When primary cosmic rays enter the atmosphere, they interact with atomic nuclei and produce a large number of secondary particles in the form of air showers. The program used to calculate the air shower is CORSIKA, which simulates the longitudinal development of the air shower by taking into account the interaction of all points. Secondary particles produced by air shower phenomena are mostly charged particles, which lose energy by exciting electrons of nitrogen in the atmosphere, and part of the energy is emitted as atmospheric fluorescence. A fluorescence model is used to estimate the amount of light in this atmospheric fluorescence. In the fluorescence model, Kakimoto [3] is used for fluorescence yield and FLASH [4] for spectra. This is used in the analysis of TA FD. Atmospheric fluorescence enters the PMT of the FD of the TA experiment after attenuation due to scattering in the propagation process in the atmosphere. From the fluorescence incident on the PMT, atmospheric scattering, incident light intensity, structures, mirror reflectance, Paraglas transmittance, BG3 filter transmittance, PMT and circuit response, etc. are taken into account to obtain the waveforms. In this way, in the simulation after the primary cosmic rays enter the atmosphere, a large number of secondary particles are produced by the air shower phenomenon, and the fluorescence emitted from the secondary particles is detected by the FD used in the TA experiment. Table 1 summarizes the conditions placed on reconstruction of events in the simulation.

Table 1: summarizes the conditions placed on reconstruction of events in the simulation.

Particle type	Proton
Number of air shower arrivals	100000
Energy	10^{18} eV, 10^{19} eV, 10^{20} eV
Zenith	0 – 65 °
Azimuth	0 – 360 °
FD station	BRM
Core position	60 km from CLF
Shower generator	CORSIKA (QGSJET-ll-04)
Atmospheric model	US standard atmosphere
Fluorescent model	Kakimoto with FLASH spectrum

In the monocular reconstruction, PMT selection, geometry reconstruction, and longitudinal developmental reconstruction are performed in the same way as in reality, and the energy and direction of arrival of primary cosmic rays are estimated. Monocular reconstruction is a technique to measure cosmic rays at a single FD station. First, Only PMTs containing atmospheric fluorescence are used in the analysis, except for PMTs that are not triggered first and PMTs triggered by night sky light, etc. Next, the plane including the shower axis and FD is determined from the trajectory of the air shower imaged by the telescope, and the geometry of the air shower is determined from the inclination of the shower axis in the plane and the time of fluorescence incidence. Finally, the longitudinal development of air showers is performed by determining the energy loss at each atmospheric depth from the amount of atmospheric fluorescence light incident on each PMT. Thus, in the monocular reconstruction, PMT selection, geometry reconstruction, and longitudinal development reconstruction are performed to estimate the energy and arrival direction of primary cosmic rays using the same method as in reality.

After performing monocular reconstruction, event selection is applied to exclude events for which geometry reconstruction is not successful. The selection conditions used in this study are listed in Table 2 [2].

Since the monocular reconstruction measures cosmic rays at a single FD station, it cannot measure the shower axis well. Therefore, the accuracy of geometry reconstruction is low, which greatly affects the accuracy of energy determination. Geometry reconstruction is one of the sources of systematic errors, and we would like to remove systematic errors other than those of the fluorescent model in this study. Therefore, we reconstruct selected events again using true geometry. Since the true geometry is used, the longitudinal developmental reconstruction is not affected by the geometry reconstruction.

Various fluorescence models were used in the reconstruction. Kakimoto, Airfly [5], AirLight [6], MACFLY [7], and Nagano [8][9] models were used as fluorescence yield models. The TA experiment uses Kakimoto et al. for the absolute fluorescence yield and FLASH for a fluorescence spectrum. We estimate the accuracy of energy determination from various models and the systematic error of atmospheric fluorescence on the reconstruction.

Table 2: Selection Conditions

Quality cuts
Number of PMTs > 10
Track length > 10°
Time extent > 2 μs
R_p > 0.5 km
Minimum viewing angle > 20°
Ψ angle < 120°
Geometrical χ^2 / ndf < 10
X_{max} inside FOV
Zenith angle < 55°
Core distance from CLF < 25 km
Energy > $10^{17.2}$ eV

3. Results

The accuracy of determining the reconstructed energy and The accuracy of determining the reconstructed X_{max} for each energy and each fluorescence model is obtained.

Figure 3 shows an example of the distribution of $\ln(\mathrm{E_{rec}}/\mathrm{E_{sim}})$, which demonstrates the error of the energy measurement and an example of the distribution of ΔX_{max}, which demonstrates the error of the X_{max} measurement. In the reconstruction using Kakimoto with FLASH model at 10^{19} eV, the accuracy of energy determination was 0.01 ± 0.08, and the accuracy of X_{max} determination was -3.4 ± 24 [g/cm^2]. The accuracy of energy and X_{max} determination was estimated to check the impact of the model change in Figure 4 on the reconstruction of each energy.

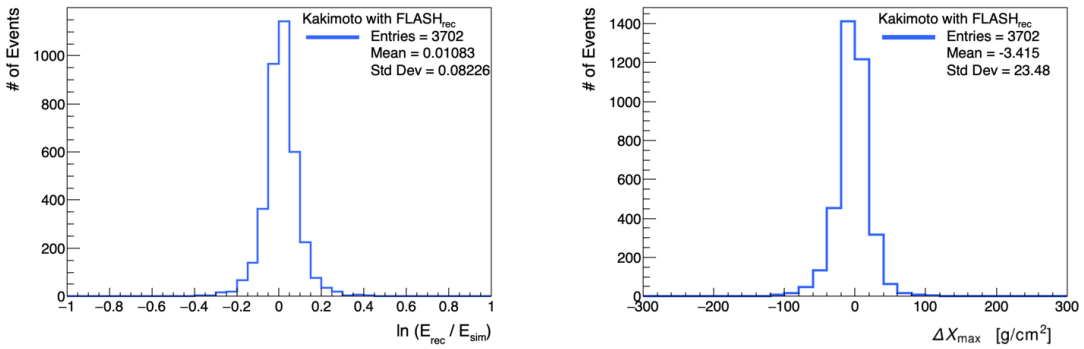

Figure 3: Left: An example of energy error distribution. Right: An example of X_{max} error distribution.

The effects of changing the model at 10^{18} eV, 10^{19} eV, and 10^{20} eV on the energy and X_{max} reconstructions are shown in Figure 4. From the left of Figure 4, when the model is changed for 10^{18} eV, 10^{19} eV and 10^{20} eV, the difference is largest between AIRFLY and MACFLY for all energies: 19 % for 10^{18} eV, 19 % for 10^{19} eV, and 18 % for 10^{20} eV. From the right side of Figure 4, the largest differences for the different models were observed between MACFLY and Nagano in 10^{18}

eV, between Kakimoto with FLASH and Nagano in 10^{19} eV and 10^{20} eV: -4.9 g/cm^2 for 10^{18} eV, -3.1 g/cm^2 for 10^{19} eV, and -2.7 g/cm^2 for 10^{20} eV.

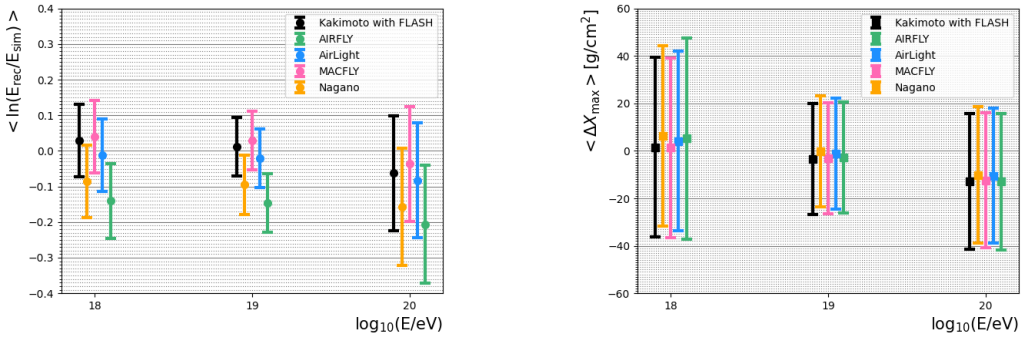

Figure 4: Left: Plot showing the effect of changing the model at 10^{18} eV, 10^{19} eV and 10^{20} eV on the energy reconstruction. Error bars are the standard deviation of the distribution of $\langle \ln(E_{rec}/E_{sim}) \rangle$. Right: Plot showing the effect of changing the model at 10^{18} eV, 10^{19} eV and 10^{20} eV on the X_{max} reconstruction. Error bars are the standard deviation of the distribution of ΔX_{max}.

Table 3 shows specific numerical values for each plot and error bar in the left-hand graph of Figure 4, and Table 4 shows specific numerical values for each plot and error bar in the right-hand graph.

Table 3: Specific values for each plot and error bar in the left graph in Figure 4

Fluorescent Model	Mean $\pm$ Std Dev (10^{18} eV)	Mean $\pm$ Std Dev (10^{19} eV)	Mean $\pm$ Std Dev (10^{20} eV)
Kakimoto with FLASH	0.03 $\pm$ 0.10	0.01 $\pm$ 0.08	-0.06 $\pm$ 0.16
AIRFLY	-0.14 $\pm$ 0.10	-0.15 $\pm$ 0.08	-0.21 $\pm$ 0.17
AirLight	-0.01 $\pm$ 0.10	-0.02 $\pm$ 0.08	-0.08 $\pm$ 0.16
MACFLY	0.04 $\pm$ 0.10	0.03 $\pm$ 0.08	-0.04 $\pm$ 0.16
Nagano	-0.09 $\pm$ 0.10	-0.10 $\pm$ 0.08	-0.16 $\pm$ 0.17

Table 4: Specific values for each plot and error bar in the right graph in Figure 4

Fluorescent Model	Mean $\pm$ Std Dev [g/cm^2] (10^{18} eV)	Mean $\pm$ Std Dev [g/cm^2] (10^{19} eV)	Mean $\pm$ Std Dev [g/cm^2] (10^{20} eV)
Kakimoto with FLASH	1.5 $\pm$ 37.8	-3.4 $\pm$ 23.5	-12.9 $\pm$ 28.6
AIRFLY	5.2 $\pm$ 42.2	-2.7 $\pm$ 23.4	-12.9 $\pm$ 28.7
AirLight	4.2 $\pm$ 37.9	-1.1 $\pm$ 23.4	-10.5 $\pm$ 28.5
MACFLY	1.3 $\pm$ 37.8	-3.1 $\pm$ 23.4	-12.5 $\pm$ 28.4
Nagano	6.23 $\pm$ 38.02	-0.3 $\pm$ 23.4	-10.2 $\pm$ 28.8

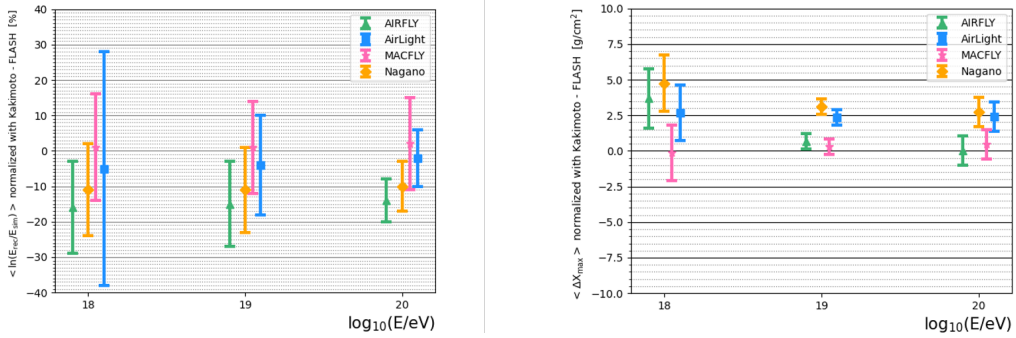

Figure 5: Left: Ratio of <ln(E_{rec}/E_{sim})>for other models to <ln(E_{rec}/E_{sim})>for Kakimoto with FLASH. (The standard is Kakimoto with FLASH). Right: Difference between <ΔX_{max}>of Kakimoto with FLASH and <ΔX_{max}>of other models. (The standard is Kakimoto with FLASH). Error bars in each plot are propagation errors.

Figure 5 shows the ratio of <ln(E_{rec}/E_{sim})>for other models to <ln(E_{rec}/E_{sim})>for Kakimoto with FLASH and the Difference between <ΔX_{max}>of Kakimoto with FLASH and <ΔX_{max}>of other models.There is an energy dependence in the reconstruction bias of energy and X_{max}. The main reason for this is considered to be the reconstruction bias of FD, since the reconstruction results of Kakimoto with FLASH model do not include atmospheric fluorescence, atmospheric conditions, and geometry uncertainties.Therefore, if the reconstruction bias is taken into account, The difference in the effect of atmospheric fluorescence yield at each energy on the determination of energy and X_{max} is about 1 percentage point for energy and 2 g/cm^2 or less for X_{max}, respectively.

4. Summary

The accuracy of determining the reconstructed energy and The accuracy of determining the reconstructed Xmax for each energy and each fluorescence model is obtained. From the left of Figure 4, when the model is changed for 10^{18} eV, 10^{19} eV and 10^{20} eV, the difference is largest between AIRFLY and MACFLY for all energies: 19 % for 10^{18} eV, 19 % for 10^{19} eV, and 18 % for 10^{20} eV. From the right side of Figure 4, the largest differences for the different models were observed between MACFLY and Nagano in 10^{18} eV, between Kakimoto with FLASH and Nagano in 10^{19} eV and 10^{20} eV: -4.9 g/cm^2 for 10^{18} eV, -3.1 g/cm^2 for 10^{19} eV, and -2.7 g/cm^2 for 10^{20} eV. From the Figure 5, There is an energy dependence in the reconstruction bias of energy and X_{max}. The main reason for this is considered to be the reconstruction bias of FD, since the reconstruction results of Kakimoto with FLASH model do not include atmospheric fluorescence, atmospheric conditions, and geometry uncertainties.Therefore, if the reconstruction bias is taken into account, The difference in the effect of atmospheric fluorescence yield at each energy on the determination of energy and X_{max} is about 1 percentage point for energy and 2 g/cm^2 or less for X_{max}, respectively.

References

[1] M. Fukushima, Status of sFLASH - Measurement of air fluorescence yield from EM shower, GCOS workshop (2022)

[2] R.U. Abbasi et al., Astroparticle Physics 80 (2016) 131 – 140

[3] F. Kakimoto et al., Nuclear Instruments and Methods in Physics Research A 372 (1996) 527-533

[4] R. Abbasi et al., Nuclear Instruments and Methods in Physics Research A 597 (2008) 37-40

[5] M.Ave et al., Astroparticle Physics 28 (2007) 41-57

[6] T. Waldenmaier, Forschungszentrum Karlsruhe - Wissenschaftliche Berichte - FZKA 7209 (2006)

[7] P. Colin et al., Astroparticle Physics 27 (2007) 317-325

[8] M. Nagano et al., Astroparticle Physics 20 (2003) 293-309

[9] M. Nagano et al., Astroparticle Physics 22 (2004) 235-248

[10] National Oceanic and Atmospheric Administration: (NOAA-S/T 76-1562): U.S. Standard Atmosphere,1976

Full Authors List: the TelescopeArray Collaboration

R.U. Abbasi[1], Y. Abe[2], T. Abu-Zayyad[1,3], M. Allen[3], Y. Arai[4], R. Arimura[4], E. Barcikowski[3], J.W. Belz[3], D.R. Bergman[3], S.A. Blake[3], I. Buckland[3], B.G. Cheon[5], M. Chikawa[6], A. Fedynitch[6,7], T. Fujii[4,8], K. Fujisue[6], K. Fujita[6], R. Fujiwara[4], M. Fukushima[6], G. Furlich[3], Z. Gerber[3], N. Globus[9*], W. Hanlon[3], N. Hayashida[10], H. He[9], R. Hibi[2], K. Hibino[10], R. Higuchi[9], K. Honda[11], D. Ikeda[10], N. Inoue[12], T. Ishii[11], H. Ito[9], D. Ivanov[3], A. Iwasaki[4], H.M. Jeong[13], S. Jeong[13], C.C.H. Jui[3], K. Kadota[14], F. Kakimoto[10], O. Kalashev[15], K. Kasahara[16], S. Kasami[17], S. Kawakami[4], K. Kawata[6], I. Kharuk[15], E. Kido[9], H.B. Kim[5], J.H. Kim[3], J.H. Kim[3†], S.W. Kim[13], Y. Kimura[4], I. Komae[4], K. Komori[17], Y. Kusumori[17], M. Kuznetsov[15,18], Y.J. Kwon[19], K.H. Lee[5], M.J. Lee[13], B. Lubsandorzhiev[15], J.P. Lundquist[3,20], T. Matsuyama[4], J.A. Matthews[3], J.N. Matthews[3], R. Mayta[4], K. Miyashita[2], K. Mizuno[2], M. Mori[17], M. Murakami[17], I. Myers[3], S. Nagataki[9], K. Nakai[4], T. Nakamura[21], E. Nishio[17], T. Nonaka[6], S. Ogio[6], H. Ohoka[6], N. Okazaki[6], Y. Oku[17], T. Okuda[22], Y. Omura[4], M. Onishi[6], M. Ono[9], A. Oshima[23], H. Oshima[6], S. Ozawa[24], I.H. Park[13], K.Y. Park[5], M. Potts[3‡], M.S. Pshirkov[15,25], J. Remington[3], D.C. Rodriguez[3], C. Rott[3,13], G.I. Rubtsov[15], D. Ryu[26], H. Sagawa[6], R. Saito[2], N. Sakaki[6], T. Sako[6], N. Sakurai[4], D. Sato[2], K. Sato[4], S. Sato[17], K. Sekino[6], P.D. Shah[3], N. Shibata[17], T. Shibata[6], J. Shikita[4], H. Shimodaira[6], B.K. Shin[26], H.S. Shin[6], D. Shinto[17], J.D. Smith[3], P. Sokolsky[3], B.T. Stokes[3], T.A. Stroman[3], Y. Takagi[17], K. Takahashi[6], M. Takamura[27], M. Takeda[6], R. Takeishi[6], A. Taketa[28], M. Takita[6], Y. Tameda[17], K. Tanaka[29], M. Tanaka[30], S.B. Thomas[3], G.B. Thomson[3], P. Tinyakov[15,18], I. Tkachev[15], H. Tokuno[31], T. Tomida[2], S. Troitsky[15], R. Tsuda[4], Y. Tsunesada[4,8], S. Udo[10], F. Urban[32], I.A. Vaiman[15], D. Warren[9], T. Wong[3], K. Yamazaki[23], K. Yashiro[27], F. Yoshida[17], Y. Zhezher[6,15], and Z. Zundel[3]

[1] *Department of Physics, Loyola University Chicago, Chicago, Illinois 60660, USA*
[2] *Academic Assembly School of Science and Technology Institute of Engineering, Shinshu University, Nagano, Nagano 380-8554, Japan*
[3] *High Energy Astrophysics Institute and Department of Physics and Astronomy, University of Utah, Salt Lake City, Utah 84112-0830, USA*
[4] *Graduate School of Science, Osaka Metropolitan University, Sugimoto, Sumiyoshi, Osaka 558-8585, Japan*
[5] *Department of Physics and The Research Institute of Natural Science, Hanyang University, Seongdong-gu, Seoul 426-791, Korea*
[6] *Institute for Cosmic Ray Research, University of Tokyo, Kashiwa, Chiba 277-8582, Japan*
[7] *Institute of Physics, Academia Sinica, Taipei City 115201, Taiwan*
[8] *Nambu Yoichiro Institute of Theoretical and Experimental Physics, Osaka Metropolitan University, Sugimoto, Sumiyoshi, Osaka 558-8585, Japan*
[9] *Astrophysical Big Bang Laboratory, RIKEN, Wako, Saitama 351-0198, Japan*
[10] *Faculty of Engineering, Kanagawa University, Yokohama, Kanagawa 221-8686, Japan*
[11] *Interdisciplinary Graduate School of Medicine and Engineering, University of Yamanashi, Kofu, Yamanashi 400-8511, Japan*
[12] *The Graduate School of Science and Engineering, Saitama University, Saitama, Saitama 338-8570, Japan*
[13] *Department of Physics, SungKyunKwan University, Jang-an-gu, Suwon 16419, Korea*
[14] *Department of Physics, Tokyo City University, Setagaya-ku, Tokyo 158-8557, Japan*
[15] *Institute for Nuclear Research of the Russian Academy of Sciences, Moscow 117312, Russia*
[16] *Faculty of Systems Engineering and Science, Shibaura Institute of Technology, Minato-ku, Tokyo 337-8570, Japan*
[17] *Graduate School of Engineering, Osaka Electro-Communication University, Neyagawa-shi, Osaka 572-8530, Japan*
[18] *Service de Physique Théorique, Université Libre de Bruxelles, Brussels, Belgium*
[19] *Department of Physics, Yonsei University, Seodaemun-gu, Seoul 120-749, Korea*
[20] *Center for Astrophysics and Cosmology, University of Nova Gorica, Nova Gorica 5297, Slovenia*
[21] *Faculty of Science, Kochi University, Kochi, Kochi 780-8520, Japan*
[22] *Department of Physical Sciences, Ritsumeikan University, Kusatsu, Shiga 525-8577, Japan*
[23] *College of Science and Engineering, Chubu University, Kasugai, Aichi 487-8501, Japan*
[24] *Quantum ICT Advanced Development Center, National Institute for Information and Communications Technology, Koganei, Tokyo 184-8795, Japan*
[25] *Sternberg Astronomical Institute, Moscow M.V. Lomonosov State University, Moscow 119991, Russia*
[26] *Department of Physics, School of Natural Sciences, Ulsan National Institute of Science and Technology, UNIST-gil, Ulsan 689-798, Korea*
[27] *Department of Physics, Tokyo University of Science, Noda, Chiba 162-8601, Japan*
[28] *Earthquake Research Institute, University of Tokyo, Bunkyo-ku, Tokyo 277-8582, Japan*
[29] *Graduate School of Information Sciences, Hiroshima City University, Hiroshima, Hiroshima 731-3194, Japan*
[30] *Institute of Particle and Nuclear Studies, KEK, Tsukuba, Ibaraki 305-0801, Japan*
[31] *Graduate School of Science and Engineering, Tokyo Institute of Technology, Meguro, Tokyo 152-8550, Japan*
[32] *CEICO, Institute of Physics, Czech Academy of Sciences, Prague 182 21, Czech Republic*

Acknowledgements

The Telescope Array experiment is supported by the Japan Society for the Promotion of Science(JSPS) through Grants-in-Aid for Priority Area 431, for Specially Promoted Research JP21000002, for Scientific Research (S) JP19104006, for Specially Promoted Research JP15H05693, for Scientific Research (S) JP19H05607, for Scientific Research (S) JP15H05741, for Science Research (A) JP18H03705, for Young Scientists (A) JPH26707011, and for Fostering Joint

∗ Presently at: University of California - Santa Cruz
† Presently at: Argonne National Laboratory, Physics Division, Lemont, Illinois 60439,USA
‡ Presently at: Georgia Institute of Technology, Physics Department, Atlanta, Geogia 30332,USA

International Research (B) JP19KK0074, by the joint research program of the Institute for Cosmic Ray Research (ICRR), The University of Tokyo; by the Pioneering Program of RIKEN for the Evolution of Matter in the Universe (r-EMU); by the U.S. National Science Foundation awards PHY-1806797, PHY-2012934, PHY-2112904, PHY-2209583, and PHY-2209584 as well as AGS-1613260, AGS-1844306, and AGS-2112709; by the National Research Foundation of Korea (2017K1A4A3015188, 2020R1A2C1008230, & 2020R1A2C2102800); by the Ministry of Science and Higher Education of the Russian Federation under the contract 075-15-2020-778, IISN project No. 4.4501.18, by the Belgian Science Policy under IUAP VII/37 (ULB), by National Science Centre in Poland grant 2020/37/B/ST9/01821. This work was partially supported by the grants of the joint research program of the Institute for Space-Earth Environmental Research, Nagoya University and Inter-University Research Program of the Institute for Cosmic Ray Research of the University of Tokyo. The foundations of Dr. Ezekiel R. and Edna Wattis Dumke, Willard L. Eccles, and George S. and Dolores Doré Eccles all helped with generous donations. The State of Utah supported the project through its Economic Development Board, and the University of Utah through the Office of the Vice President for Research. The experimental site became available through the cooperation of the Utah School and Institutional Trust Lands Administration (SITLA), U.S. Bureau of Land Management (BLM), and the U.S. Air Force. We appreciate the assistance of the State of Utah and Fillmore offices of the BLM in crafting the Plan of Development for the site. We thank Patrick A. Shea who assisted the collaboration with much valuable advice and provided support for the collaboration ' s efforts. The people and the officials of Millard County, Utah have been a source of steadfast and warm support for our work which we greatly appreciate. We are indebted to the Millard County Road Department for their efforts to maintain and clear the roads which get us to our sites. We gratefully acknowledge the contribution from the technical staffs of our home institutions. An allocation of computing resources from the Center for High Performance Computing at the University of Utah as well as the Academia Sinica Grid Computing Center (ASGC) is gratefully acknowledged.